Electric-field effects on intersubband Raman laser gain in modulation-doped GaAs/AlGaAs coupled double quantum wells

Makoto Miura * , Shin'ichi Katayama

School of Materials Science, Japan Advanced Institute of Science and Technology, 1-1 Asahidai, Nomi, Ishikawa 923-1292, Japan

Abstract

We study numerically the electric-field effects on optically pumped mid-infrared intersubband Raman lasers (IRL) consisting of modulation-doped GaAs/AlGaAs asymmetric coupled double quantum wells. The collective plasmon nature of intersubband excitations is important to analyze the characteristics of IRL gain. The lasing wavelength is changed from 15.0 to 12.5 μm by increasing applied bias from -40 to 10 kV/cm for pumping wavelength 9.56 μm with intensity 250 kW/cm^2 if the maximum gain at threshold ($G_{R_{th}}^{max} = \alpha/\Gamma_{opt}$) was assumed to be 100cm^{-1}, α and Γ_{opt} being total radiation loss and optical confinement factor, respectively.

Key words: Intersubband Raman laser ; Asymmetric coupled double quantum wells

1 Introduction

Since the invention of quantum cascade lasers[1], finding the novel tunable infrared lasers based on semiconductor quantum well structures has attracted our attention because of increasing requirements for trace gas analysis, remote chemical sensing and laser radar etc. Recently, Liu et al. [2] have succeeded in the observation of optically pumped intersubband Raman laser (IRL) in the wavelength from 10 to 15 μm in modulation doped n-type GaAs/AlGaAs asymmetric coupled double quantum wells (ACDQWs). Further, later experiments [3] have revealed a new feature of the emission energy. The observed

* Tel.: +81-761-51-1510; fax: +81-761-51-1515
Email address: mk-miura@jaist.ac.jp (Makoto Miura).

lasing energy does not correspond well to the intersubband (ISB) transition energy which was predicted by Khurgin et al. [4], but it appears at the ISB plasmon energy coupled to the longitudinal optical (LO) phonons. This suggests us that the ISB transitions should be considered as collective rather than the single-particle excitations due to the interactions between electron-electron and electron-LO phonons. Based on the light scattering theory due to ISB charge-density-excitation (CDE) mechanism, Maung and Katayama have explained well the experimental data, taking into account the coupling of electrons with the confined and interface phonon modes [5,6].

In this paper, we explore the electric field effects on IRL gain and lasing wavelength toward realizing of IRL which is controlled by an external bias field. The first study of IRL in an applied bias has been carried out by Sun et al. [7], but they did not concern the importance of collective nature of ISB excitations. We demonstrate a clear evidence of bias field on the maximum Raman gain and emission wavelength of GaAs/AlGaAs IRL by calculating the proper depolarization field effects on the Raman gain spectrum.

This paper is organized as follows. In section 2, model and calculation method are described. In section 3, results and discussion are given. Section 4 is devoted to a brief summary.

2 Model and method of calculation

In Fig. 1(a), we show a schematic view of IRL device, in which the side pumping and Stokes emission from the two facets are necessery for the lasing of transverse magnetic mode. Figure 1(b) shows the two-step resonant electronic Raman scattering due to the ISB charge density excitations in ACDQWs. In the scattering process, the pump photon excites an electron from the ground state E_1 to the excited state E_3 virtually with appropriate detuning, and the subband transition from the excited state E_3 to lower state E_2 emits the Stokes photon accompanied by the ISB charge-density-fluctuations. Thus the Stokes shift energy corresponds to the collective intersubband excitation between state E_1 and state E_2.

According to ref.[5], the IRL gain of single ACDQWs is expressed by

$$G_R = \frac{4\pi^3 c^2}{\omega_i \omega_s^2 \varepsilon_s} (N_1 - N_2) \left\{ \frac{d^2\sigma}{d(\hbar\omega)\, d\Omega} \right\} I_{pump} \ , \tag{1}$$

where I_{pump} is the pump intensity, ω_i (ω_s) is the pump (emitted) photon frequency, N_i is the population for i-th subband, and ε_s is dielectric constant at scattered photon frequency, respectively. Thus, the Stokes shift frequency is

given by $\omega = \omega_i - \omega_s$. The spectral differential scattering cross section due to the collective ISB excitations in the CDE mechanism is

$$\frac{d^2\sigma}{d\omega d\Omega} = -\frac{r_0^2\hbar}{\pi n_s}\left(\frac{\omega_s}{\omega_i}\right)|R(1,2)|^2\left[n(\omega)+1\right]\mathrm{Im}\left\{\chi_{11}(q,\omega)\right\} \ , \tag{2}$$

where n_s is the 2D electron sheet density, $r_0 = e^2/(m^*c^2)$ is the classical radius of an electron having effective mass m^*, and $n(\omega)$ is the Bose-Einstein distribution factor [5]. $R(1,2)$ is the Raman tensor component as

$$R(1,2) = -m^*\omega_{32}\omega_{31}Z_{32}Z_{31}\left(\frac{1}{-\delta+i\Gamma}\right) \ , \tag{3}$$

where $\hbar\omega_{ij}(=E_{ij}) = E_i - E_j$, $\delta\,(=E_{31}-\hbar\omega_i)$ denotes the detuning of pump laser and Γ is the linewidth of intersubband transition. Z_{ij} is the dipole matrix element $Z_{ij} = \langle\psi_i|z|\psi_j\rangle$, with the envelope wave function of i-th subband ψ_i. The quantity χ_{11} is a dynamical response function which was calculated by taking into account the many-body electron-electron and electron-confined LO (interface) phonon in random phase approximation (RPA). The explicit form of χ_{11} becomes

$$\chi_{11}(q,\omega) = \frac{\chi^0(\omega)}{1 - V_{11}^{eff}(q,\omega)\,\chi^0(\omega)} \ , \tag{4}$$

with the effective electron-electron interaction

$$V_{11}^{eff}(q,\omega) = V_{11}^{Coul} + V_{11}^{e-ph} \ . \tag{5}$$

In the above Eq. (5) , the first Coulomb term is

$$V_{11}^{Coul} = \frac{4\pi e^2}{\varepsilon_\infty}L_{11} \ , \tag{6}$$

with the optical dielectric constant ε_∞, and

$$L_{11} = \int_{-\infty}^{\infty}\left[\int_0^z \psi_1(z)\,\psi_2(z_1)\,dz_1\right]\left[\int_0^z \psi_2(z)\,\psi_1(z_2)\,dz_2\right]dz \ . \tag{7}$$

The second term in Eq. (5) is the effective electron-electron interaction via the coupling of electron with various phonon modes as

$$V_{11}^{e-ph} = \sum_{\nu} \frac{2\hbar\omega_{q,\nu}}{\hbar^2\left(\omega^2 - \omega_{q,\nu}^2\right)} \int_{-\infty}^{\infty} dz_1 \int_{-\infty}^{\infty} dz_2 \psi_1(z_1)\psi_2(z_1) \times \phi_{\nu}^{ph^*}(q, z_1)\phi_{\nu}^{ph}(q, z_2)\psi_2(z_2)\psi_1(z_2) \quad . \tag{8}$$

In Eq. (8), ν denotes the mode index of phonons, $\omega_{q,\nu}$ is the frequency of phonon mode ν, and $\phi_{\nu}^{ph}(q, z)$ is electrostatic potential of mode ν.

In present work, we solve at first the Schrödinger-Poisson equations numerically in the presence of external electric field. The estimated subband energy and wave functions are utilized for evaluation of R and χ_{11}. V_{11}^{e-ph} is estimated by using electrostatic potential for each phonon mode and electoronic wave functions. The dispersion relation and corresponding electrostatic potential associated with the interface modes are evaluated by means of transfer matrix method. According to these procedures the maximum IRL gain is determined as a function of applied electric field, and lasing frequency is estimated by assuming appropriate value of the ratio between IRL optical loss and optical confinement factor.

3 Results and discussion

In Fig. 2, we plot the calculated energy separation of subbands E_{ij} $(i > j\,(= 1, 2, 3))$ versus electric field for GaAs/$Al_{0.3}Ga_{0.7}As$ ACDQWs structure at 80 K. The inset shows our modeled ACDQWs with well width 7.5 and 6.0nm coupled by a thin barrier (1.13nm) surrounded by thick barriers(10.0nm). We assume electron effective mass to be $0.067m_0$ and optical dielectric constant 10.89 in GaAs, and $0.085m_0$ and 10.07 in $Al_{0.3}Ga_{0.7}As$, respectively. [8] It is also supposed that the Si donors are doped at center of thick barrier with $n_d = 1.5 \times 10^{18}cm^{-3}$, so that the 2D sheet density is $n_s = 3 \times 10^{11}cm^{-2}$ at 80 K. From Fig. 2, it is evident that E_{21} depends strongly on bias field while E_{31} is almost independent of the field strength. In ref. [5], it was pointed out that the poles of χ_{11} give two prominent peaks due to the coupled ISB plasmon-phonon modes (upper branch: I^+, lower branch: I^-) in a gain spectrum, in addition to the weak peaks originating from the coupled ISB plasmon-interface phonon modes.

In Fig. 3, the values of the maximum Raman gain (G_R^{max}) are plotted by the dashed and solid line for I^- and I^+ modes as a function of bias field. In this calculation of G_R^{max}, we set $N_1 - N_2 \simeq N_1$ by assuming $N_1 \gg N_2$ in Eq.(1). The quantities I_{pump}, pump wavelength, Γ and δ are assumed to be 250 kW/cm^2, 9.56 μm, 10.0 meV and 15.1 meV, respectivery. We chose those so as to optimize the Raman gain in zero bias. The maximum Raman gain of

the I^- mode has a broad peak near -10 kV/cm as a function of electric field, whereas the one for I^+ mode increases from zero to 470 cm^{-1} as the bias field decreases.

We know that lasing may occur when the G_R^{max} dominates the absorption coefficient α describing radiation losses in IRL such as mirror loss, excited carrier-ionized impurity and carrer-interface roughness scatterings etc. Thus the threshold condition for Stokes lasing is defined by

$$\Gamma_{opt} G_{R_{th}}^{max} = \alpha, \tag{9}$$

where Γ_{opt} denotes the optical confined factor. In the present analysis, we assume $G_{R_{th}}^{max} = \alpha/\Gamma_{opt}$ to be 100 cm^{-1} according to Sun et al. [7] which is denoted by thin cross bar in Fig. 3. From the comparison of maximum gain with $G_{R_{th}}^{max}$, the Raman lasing takes place for a range from -40 to 10 kV/cm. In the previous work [5], it was shown that the superior mode in the maximum Raman gain should exhibit the Raman lasing action. It is expected that the lasing of Stokes scattered light due to the I^- and I^+ mode interchanges at -20 kV/cm from the bold dashed line(I^-) to the bold solid one (I^+) as bias decreases. The calculated Stokes lasing wavelength is shown as a function of electric field in Fig. 4. The bold dashed and solid line denote the output Stokes wavelength related to the I^- and I^+ mode. We find that the applied bias changing from -40 to 10 kV/cm is able to vary the lasing wavelength from 15.0 to 12.5 μm. It is predicted that a jump of laser wavelength from 12.8 to 13.7 μm exists at -20 kV/cm.

The dependence of G_R^{max} on electric field is coming from those of $R(1,2)$ and $\mathrm{Im}(\chi_{11})$ as is seen in Eq. (2). Although we do not show explicitly the detail of numerical values, $\mathrm{Im}(\chi_{11})$ gives rise to apparent dependence on bias compared with that of $R(1,2)$ from 10 to -40 kV/cm. As is pointed out above, the maximum Raman gain associated with I^+ mode below -40 kV/cm might increase monotonously. But we expect the monotonous increase ceases due to the reduction of Z_{31} and Z_{32} in $R(1,2)$ because the wavefunction of subband 3 should expand from the well in such a strong electric field.

Finally, we give two brief comments related to our approximation. The first one is that, though we set $N_1 - N_2 \simeq N_1$ in Eq.(1), it should be determined self-consistently by solving the coupled rate equations for N_1, N_2 and number of stimulated Stokes photon with appropriate relaxation times. The second one is related to our single ACDQWs model. The experiments were carried out in samples consisting of multiple ACDQWs[3], and it is known that the lasing condition in Eq.(9) depends on the number of wells and total radiation loss related to waveguide structures. The optimum number of wells should be evaluated to realize the IRL with efficient tune of wavelength by applied bias.

4 Sumarry

We have explored the electric field effects on the intersubband Raman laser gain in modulation-doped n-type GaAs/AlGaAs ACDQWs based on the numerical calculation of electronic states and phonon modes with emphasis on the coupling between the ISB plasmon and confined LO phonon. It is demonstrated that the applied electric field bias changing from -40 to 10 kV/cm is able to vary the lasing wavelength from 15.0 to 12.5 μm by assuming $G_{R_{th}}^{max} = \alpha/\Gamma_{opt}$ to be 100 cm^{-1}, while the IRL wavelengths distributed from 10 to 15 μm were observed in many samples with various well widths in the experiments of IRL [3]. The present results provide important information of possible tunable IRL as well as the voltage-controlled frequency modulator in mid-infrared frequency regime.

Acknowledgement

The authors thank Dr. S. M. Maung for designing prototype of programs for simulations.

References

[1] J. Faist, F. Capasso, D. L. Sivco, C. Sirtori, A. L. Hutchinson and A. Y. Cho, Quantum Cascade Laser, Science, 264(1994), pp. 553-556

[2] H. C. Liu, I. W. Cheung, A. J. SpringThorpe, C. Dharma-wardana, Z. R. Wasilewski, D. J. Lockwood and G. C. Aers, Intersubband Raman Laser, Appl. Phys. Lett., 78(2001), pp. 3580-3582

[3] H. C. Liu, C. Y. Song, Z. R. Wasilewski, A. J. SpringThorpe, J. C. Cao, C. Dharma-wardana, G. C. Aers, D. J. Lockwood and J. A. Gupta, Coupled Electron-Phonon Modes in Optically Pumped Resonant Intersubband Lasers, Phys. Rev. Lett., 90(2003), 077402

[4] J. B. Khurgin, G. Sun, L. R. Friedman and R. A. Soref, Comparative analysis of optically pumped intersubband lasers and intersubband Raman oscillators, J. Appl. Phys., 78(1995), pp. 7398-7400

[5] S. M. Maung and S. Katayama, Theory of Intersubband Raman Laser in Modulation-doped Asymmetric Coupled Double Quantum Wells, J. Phys. Soc. Jpn., 73(2004), pp. 2562-2570

[6] S. M. Maung and S. Katayama, Theory of Raman Lasing due to Coupled intersubband Plasmon-Phonon Modes in Asymmetric Coupled Double Quantum Wells, Proc. 27th Int. Conf. Phys. Semicon., AIP, 2005, pp. 945-946

[7] G. Sun, J. B. Khurgin, L. Friedman and R. A. Soref, Tunable intersubband Raman laser in GaAs/AlGaAs multiple quantum wells, J. Opt. Soc. Am. B, 15(1998), pp. 648-651

[8] S. Adachi, GaAs, AlAs, and $Al_xGa_{1-x}As$: Material parameters for use in research and device applications, J. Appl. Phys., 58(1985), pp. R1-29

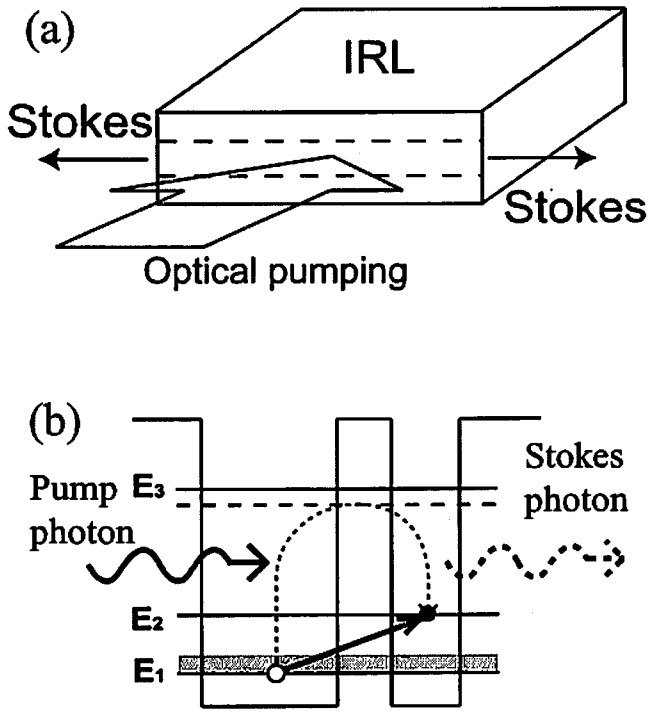

Fig. 1. (a) Geometry of IRL device. (b) CDE mechanism of ISB excitation.

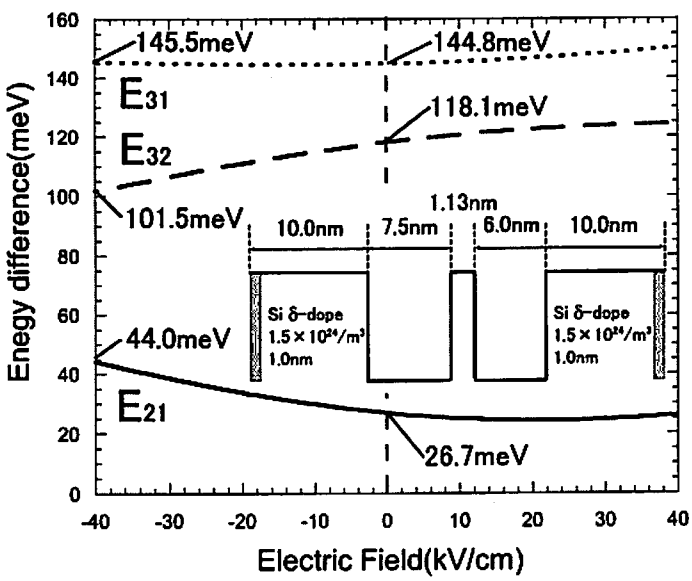

Fig. 2. Subband energy separation versus electric field in GaAs/$Al_{0.3}Ga_{0.7}As$ (Inset shows ACDQWs structure.)

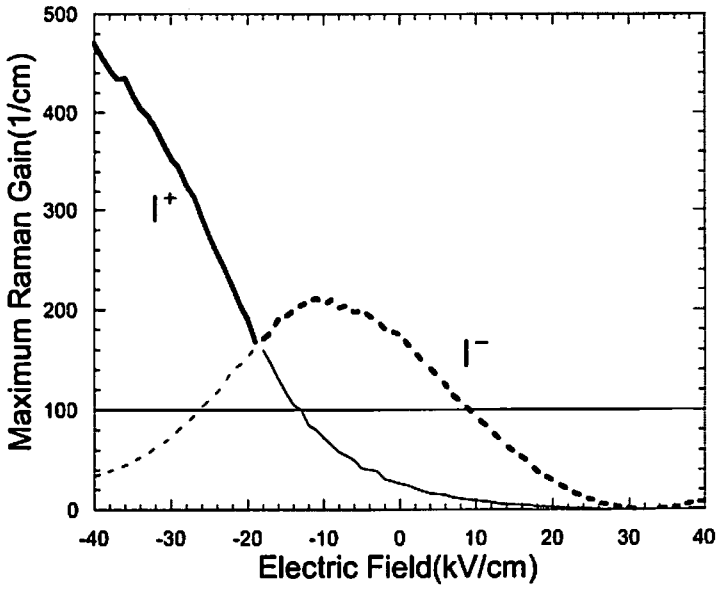

Fig. 3. Electric-field dependence of maximum Raman gain for the coupled plasmon-confined LO phonon modes. (The bold dashed and solid line correspond to the I^- and I^+ mode.)

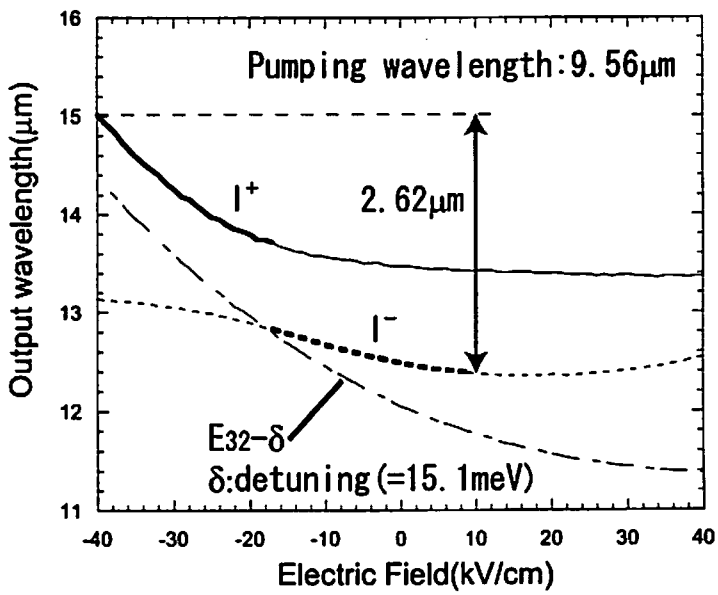

Fig. 4. Electric-field dependence of IRL output wavelength.(The bold dashed and solid line correspond to the I^- and I^+ mode.)